8 P

CR

IN-28715

Dr. Gilbert Mead
Code 601
Crustal Dynamics Program
Space and Earth Science Directorate
Goddard Space Flight Center
Greenbelt, MD 20771

October 3, 1986

Dear Dr. Mead,

Enclosed please find three copies of a semi-annual status report for NASA grant NAG 5-750, Viscoelastic Deformation Near Active Plate Boundaries.

Sincerely,

Steven N. Ward

cc: NASA Scientific and Technical Information Facility
Genevieve Wiseman, NASA Grants Officer

(NASA-CR-179726) VISCOELASTIC DEFORMATION NEAR ACTIVE PLATE BOUNDARIES Semiannual Status Report (California Univ.) 8 p CSCL 08G
N86-32909
Unclas
G3/46 44621

Viscoelastic Deformation Near Active Plate Boundaries

NAG 5-750

Steven N. Ward
C.F. Richter Laboratory
Earth Science Board
University of California
Santa Cruz, CA 95064

Investigation: Model deformations near the active plate boundaries of Western North America using space-based geodetic measurements as constraints.

Status: The first six months of this project were spent gaining familiarity with space-based measurements, accessing the Crustal Dynamics Data Information Computer, and building time independent deformation models. The initial goal is to see how well the simplest elastic models can reproduce VLBI baseline data.

Results: From the Crustal Dynamics Data Information Service, a total of 18 VLBI baselines are available which have been surveyed on four or more occasions (see Figure 1). These data were fed into weighted and unweighted inversions to obtain baseline closure rates. Figure 2 illustrates four of the better quality lines.

The deformation model assumes that the observed baseline rates result from a combination of rigid plate tectonic motions plus a component resulting from elastic strain build up due to a failure of the plate boundary to slip at the full plate tectonic rate. The elastic deformation resulting from the 'locked' plate boundary is meant to portray interseismic strain accumulation. During and shortly after a large interplate earthquake, these strains are largely released, and points near the fault which were previously retarded suddenly catch up to the positions predicted by rigid plate models. Figure 3 illustrates the predicted velocity field from a model which includes predicted RM2 plate velocities divided equally between the North American and the Pacific plate, and the interseismic strain accumulation due to a locked plate boundary of 50 *km* thickness.

How well do such simple models fit the observed VLBI baselines? We judge the quality of fit by the sum squares of weighted residuals, termed total variance. The observed baseline closures (Table 1, column 1) have a total variance of 99 $(cm/y)^2$. When the RM2 velocities are assumed to model the data (column 2), the total variance increases to 154 $(cm/y)^2$. For California, the assumption of rigid plate motion is actually worse than the assumption of no motion at all. In contrast, the total variance for the 50 *km* locked elastic model is 43 $(cm/y)^2$ (Table 1, column 3). With a 56% reduction in data variance, we are lead to believe that elastic models of this type probably can account for the majority of the VLBI signal.

What specifics can the VLBI baseline closures reveal about the North American-Pacific plate boundary? Two parameters which might be extracted from the data are the thickness of the plate boundary and the degree of locking. Generally, the deeper the plate boundary, the wider the zone of deformation. Likewise, the less the degree of locking, the thinner the zone of deformation. Figure 4 contours variance of fit versus boundary thickness and degree of locking. The degree of locking is quoted in terms of right lateral slip rate. A slip rate of 0 cm/y means a fully locked boundary. A slip rate of 5.6 cm/y would be a completely unlocked boundary. For shallow plate boundaries (≈50 *km*), the best models are totally locked. With increasing boundary thickness, the best models slip at about 1/4 of the total interplate rate. This seems reasonable, as deeper portions of the boundary probably are slipping at a faster rate than shallower portions. The best models have interplate boundaries about 240 *km* thick which slip at rates of about 1.5 cm/y. The best model has a total variance of 27 $(cm/y)^2$ and fits the data 37% better than the 50 *km*, totally locked model of Figure 3.

Figure 5 illustrates the effects of plate boundary depth and degree of locking on the width of the deformation zone. Maps in Figure 5 contour the magnitude of plate velocity in cm/y relative to a fixed point distant from the fault on the Pacific Plate. The left column is computed for totally locked plate boundries of 250, 160 and 70 *km* thickness. For locked boundaries, the width of the interplate deformation zone is about three times the locked depth. The right hand column contours the velocities for a boundary of 250 *km* depth with creeps at 0, 1.1, and 2.2 cm/y. Note that the behavior of these two different model sequences is very similar. This tradeoff in parameters will require a large data set to differentiate.

Reports: Results of this work will be presented in a talk entitled 'California Deformation Models from VLBI Data' to be given at the 1986, Fall Meeting of the Crustal Dynamics Investigators, Goddard Space Flight Center, Greenbelt, Maryland.

BASELINE		BASELINE RATE (CM/YR) OBS	RM2	CALC
OVRO 130	JPL 7263	-2.324	-4.452	-2.127
OVRO 130	VANDENBERG 7223	0.242	-1.790	-1.201
OVRO 130	MOJAVE	-0.305	0.000	-0.156
OVRO 130	PEARBLOSSOM	-0.802	0.000	-1.681
OVRO 130	MONUMENT PEAK	-2.078	-5.113	-2.633
OVRO 130	PALOS VERDES	-0.531	-4.277	-2.840
OVRO 130	PINYON FLATS	-0.219	0.000	-1.284
JPL 7263	VANDENBERG 7223	2.923	0.000	1.178
JPL 7263	MOJAVE	1.662	-0.910	-0.077
VANDENBERG 7223	MOJAVE	0.867	2.117	1.960
VANDENBERG 7223	PINYON FLATS	2.751	4.447	2.595
HAT CREEK	MOJAVE	-0.609	0.000	-0.207
MOJAVE	MONUMENT PEAK	-0.349	-4.707	-2.238
MOJAVE	PINYON FLATS	0.076	0.000	-1.016
DSS 13	JPL 7263	-0.527	-0.502	0.121
OVRO 130	HAT CREEK	0.656	0.000	-0.054
MOJAVE 12	HAT CREEK	0.302	0.000	-0.206
OVRO 130	MOJAVE 12	-0.215	0.000	-0.154
TOTAL WEIGHTED VARIANCE (CM/YR)**2		98.66	154.40	42.92

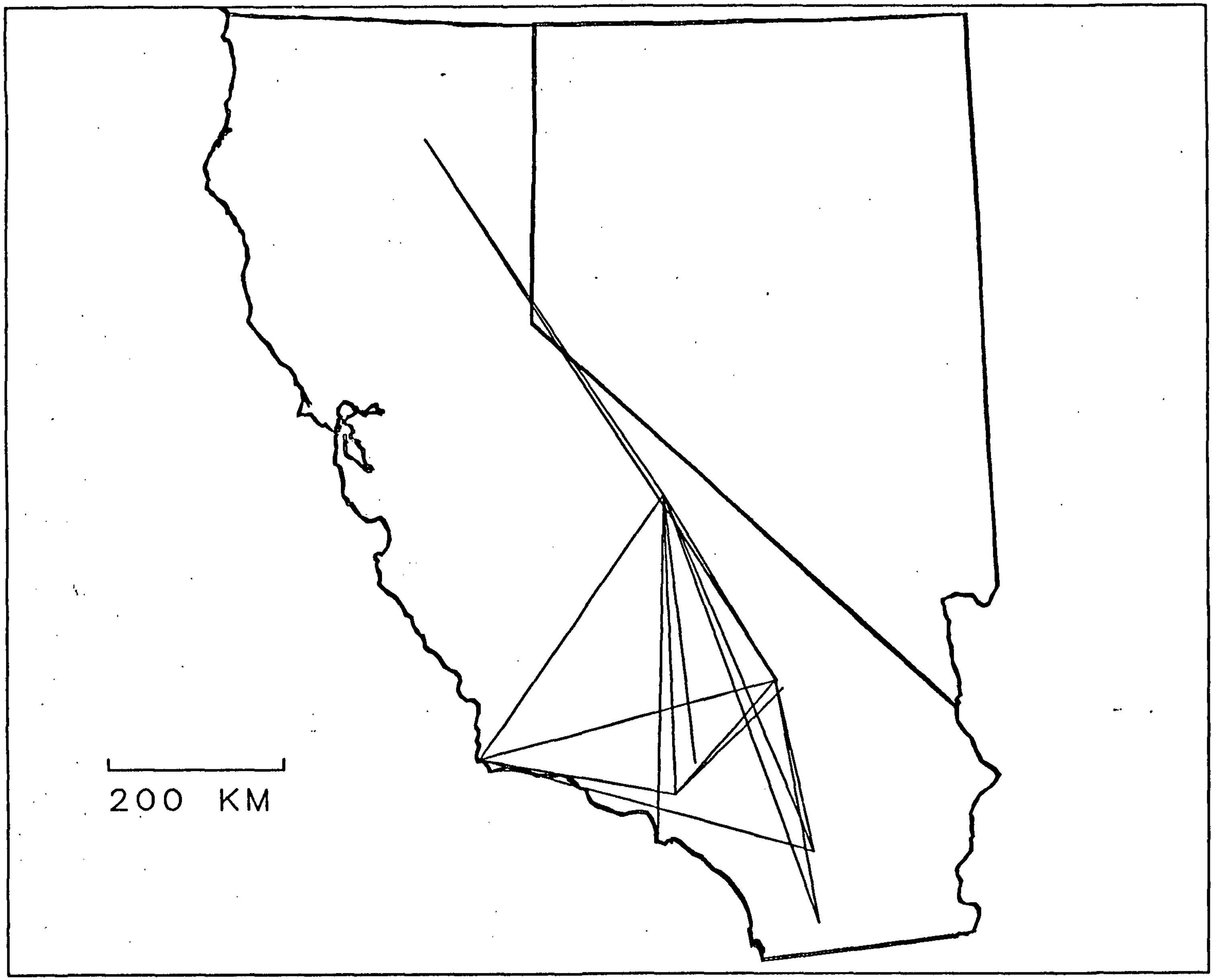

Figure 1) Map showing California VLBI baselines available from the Crustal Dynamics Information Service which have four or more surveys.

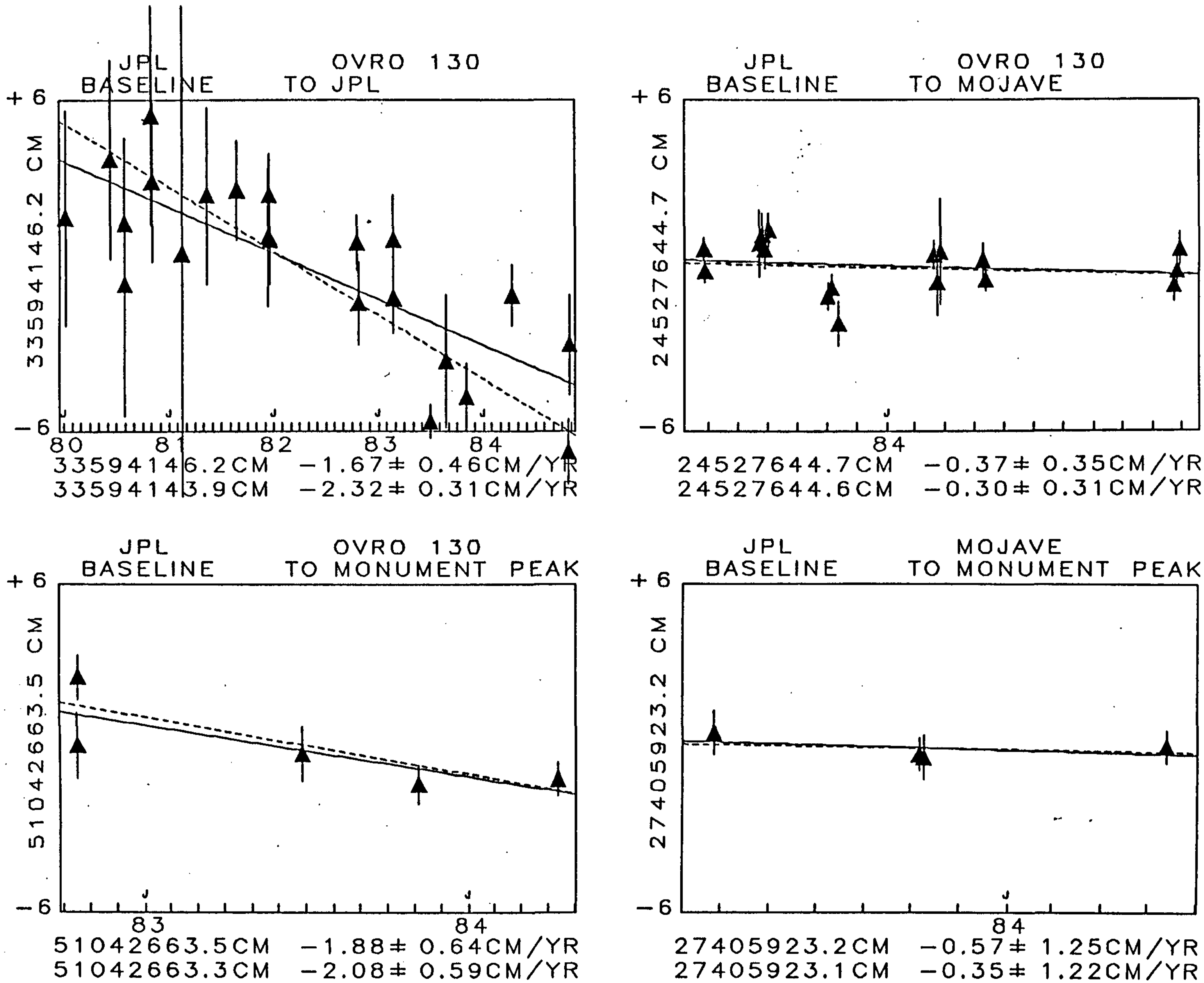

Figure 2) Samples of typical 'good' data. Solid and dashed lines are unweighted and weighted linear fits to the data.

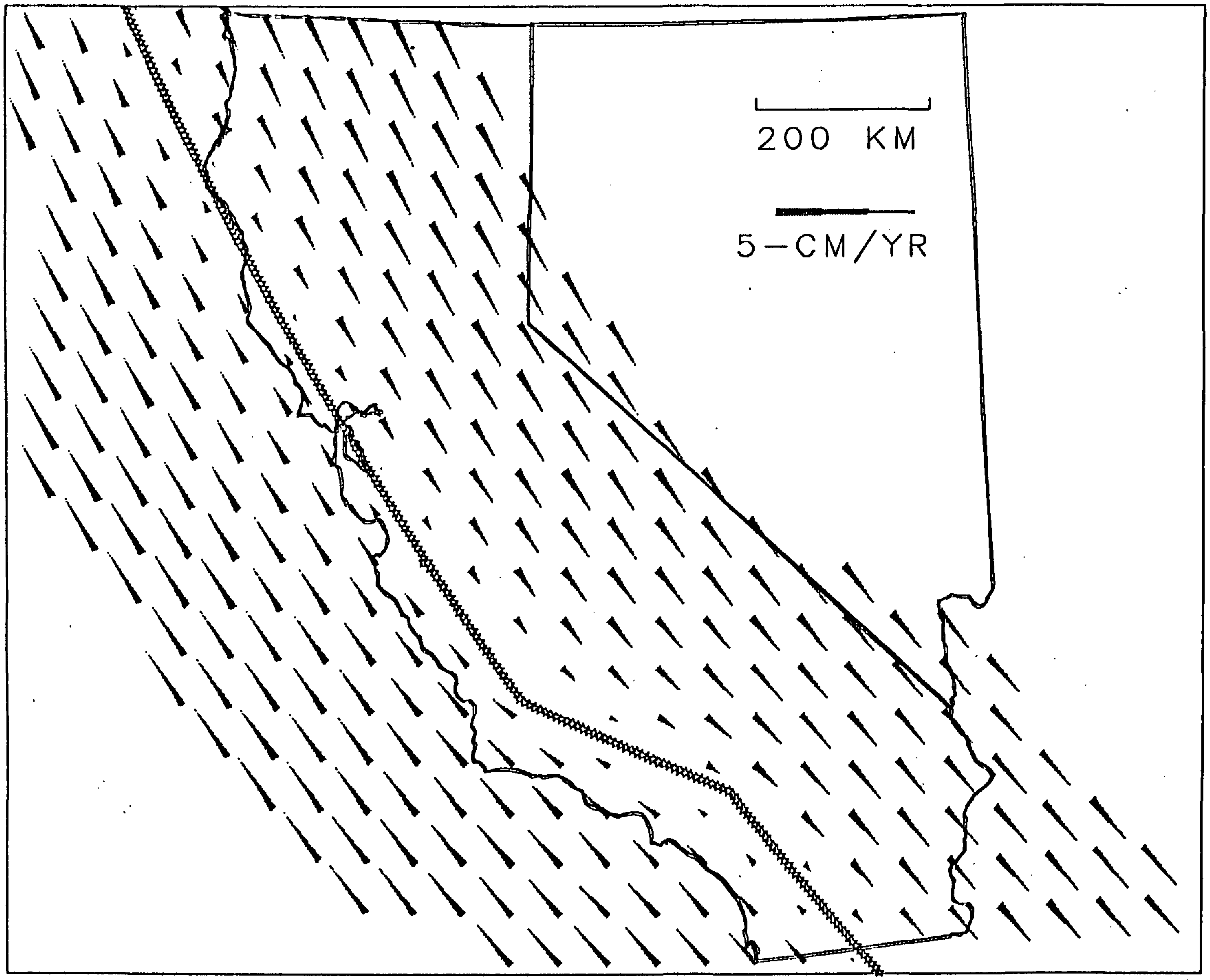

Figure 3) Map showing computed velocities for an elastic model which includes a completely locked plate boundary of 50 *km* thickness.

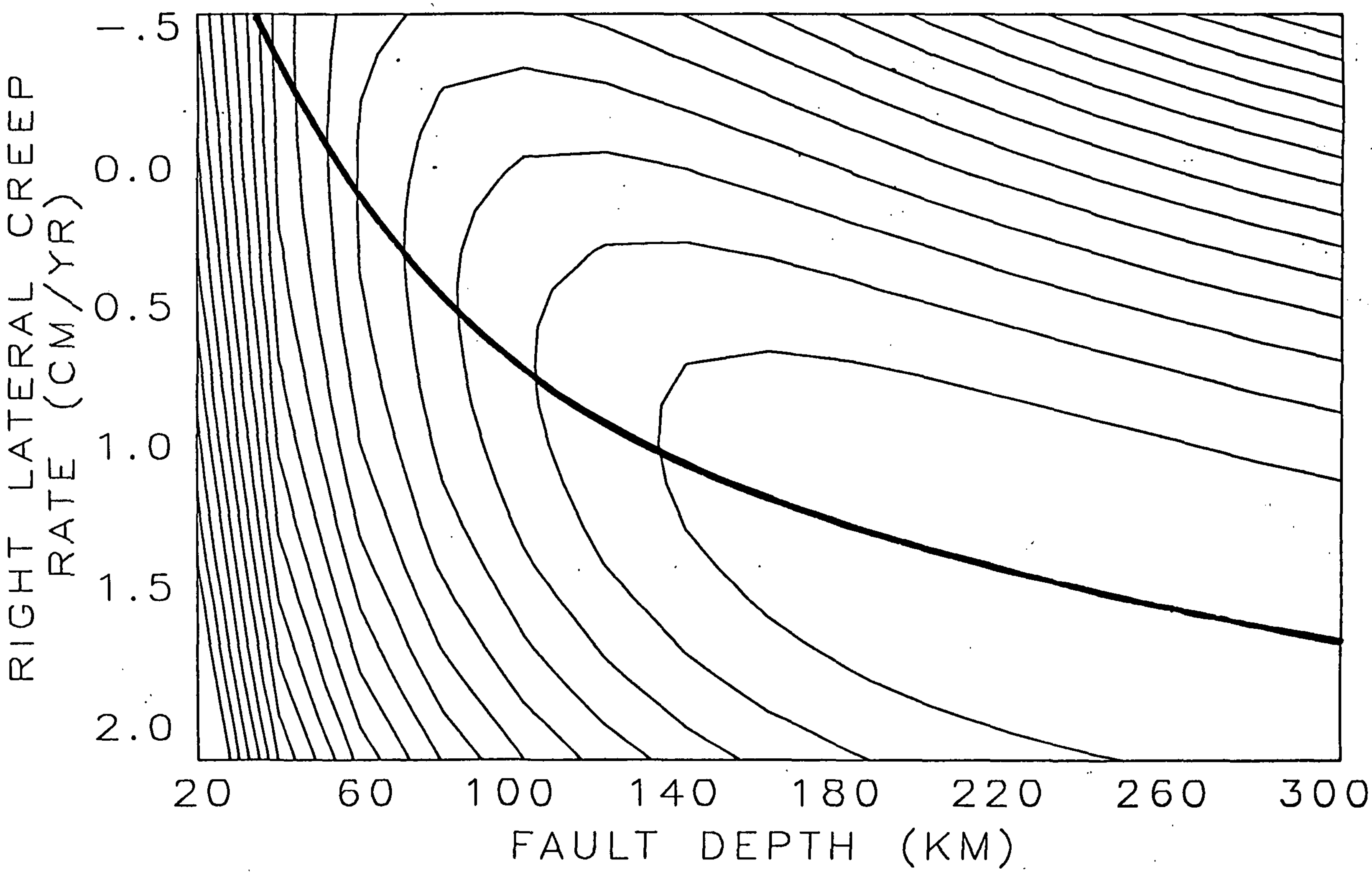

Figure 4) Contours of total variance versus plate boundary thickness and degree of locking. The dark curve traces the best degree of locking given an assumed boundary thickness. Thicker plate boundries require a lesser degree of locking.

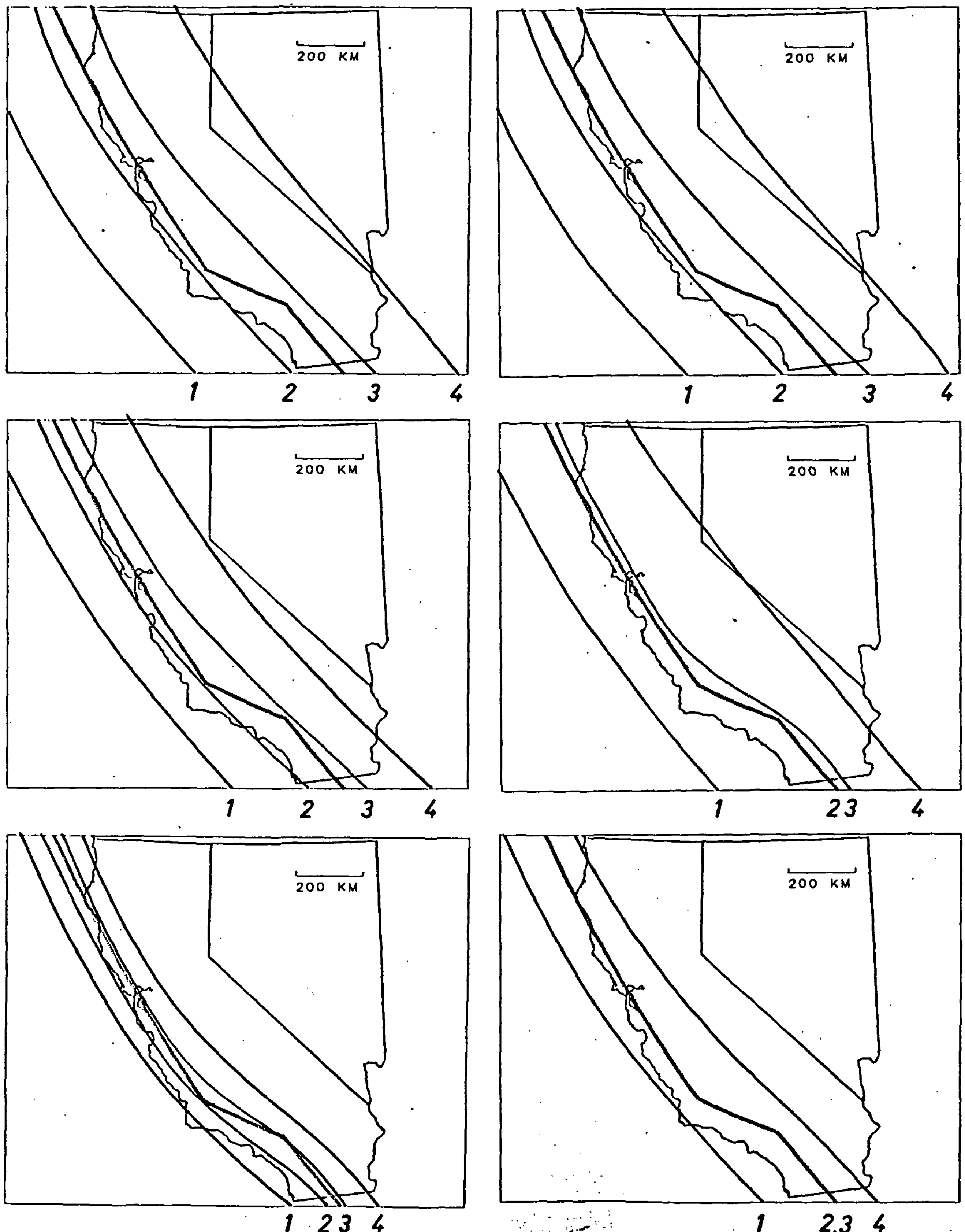

Figure 5) Maps illustrating the tradeoff between boundary thickness and degree of locking. Increasing boundary thickness for a fixed degree of locking (left) and increasing degree of locking for a fixed boundary thickness (right) have very similar effects.